Laser-Guide Star Point-Spread Function Reconstruction for Extremely Large Telescopes

C. Correia[a,*], J.-P. Véran[a], B. Ellerbroek[b], L. Gilles[b] and L. Wang[b]

[a]Herzberg Institute of Astrophysics, National Reserarch Council, Canada
[b] Thirty Meter Telescope Observatory Corporation, Suite 200, 1111 S. Arroyo Parkway, Pasadena CA, USA
[*]carlos.correia@nrc.gc.ca

Abstract. This paper discusses a simulation-based framework for laser guide star (LGS) point spread function reconstruction (PSFR) for the *Thirty Meter Telescope's* 1[st]-light multi-conjugate adaptive optics system NFIRAOS. The approach is based on processing first the NFIRAOS on-axis LGS measurements to compute a tip/tilt-removed (TTR) LGS structure function (SF) using Véran's method. This reconstructed LGS SF can then be used to estimate the PSF in science directions as discussed in [Gilles et al., 2011] in this same conference.

1 Introduction

To exploit the maximum potential of Extremely Large Telescopes (ELT), adaptive-optics (AO)-corrected images can be further enhanced by using image deconvolution techniques. Such techniques rely on accurate knowledge of the point-spread function (PSF) anywhere in the field.
On the other hand, to increase sky-coverage ELTs use laser beacons (LGS) to probe the three-dimensional atmosphere and multi-conjugate AO to increase correction beyond the isoplanatic patch. Both these features translate into three sources of anisoplanatism: 1) focal anisoplanatism known as cone effect 2) angular anisoplanatism due to the difference of the wave-fronts in the LGS and science directions and 3) tip/tilt (TT) angular anisoplanatism, on account of the LGS wave-front sensors (WFS) being blind to TT, the latter being estimated from multiple natural guide star measurements in different locations in the field.
In our approach, the long-exposure science OTF, which is the Fourier transform of the PSF, is estimated as a product of 2 terms: (i) a tip-tilt-removed science OTF estimated from system telemetry using Véran's method and a model anisoplanatism SF filter, computed from a high-fidelity numerical simulation to account for the range and angular separation difference between the location of the LGS and the science target and (ii) a tip/tilt science OTF obtained from system and model telemetry by processing multiple low-order WFS data.
We present the first stage of the reconstruction, *i.e.* the LGS PSF reconstruction, the remainder – TTR and TT anisoplanatic filters – being presented by [Gilles et al., 2011]. Based on [Véran et al., 1997], we show how to reconstruct the LGS PSF by de-noising system telemetry and removing AO-loop specific terms, in particular aliasing; the modifications needed on account of the system size and the optimisations required to accurately reconstruct the PSF are outlined. Furthermore, PSF estimates are compared to those of a high-fidelity Monte-Carlo simulator (MAOS) [Wang et al., 2011] available from `https://github.com/lianqiw/maos` that can accurately model the PSF in those locations. Performance metric used is Strehl-ratio.

2 [Véran et al., 1997] method revisited

[Véran et al., 1997] proposed a method for estimating the PSF from closed-loop telemetry that can be phrased as follows:

What would be the residual phase measured by an ideal wave-front sensor (WFS) that would not be affected by measurement nor aliasing errors?

In practice, a Hartmann-Shack (HS)-WFS measures the gradient of the phase, not the phase. Moreover, measurements are corrupted by measurement noise and aliasing, whose influence on the residual phase must be subtracted from the actual WFS measurements to estimate the residual phase that an ideal WFS would have access to. Figure 1 depicts the principle of operation that underlies the PSF reconstruction.

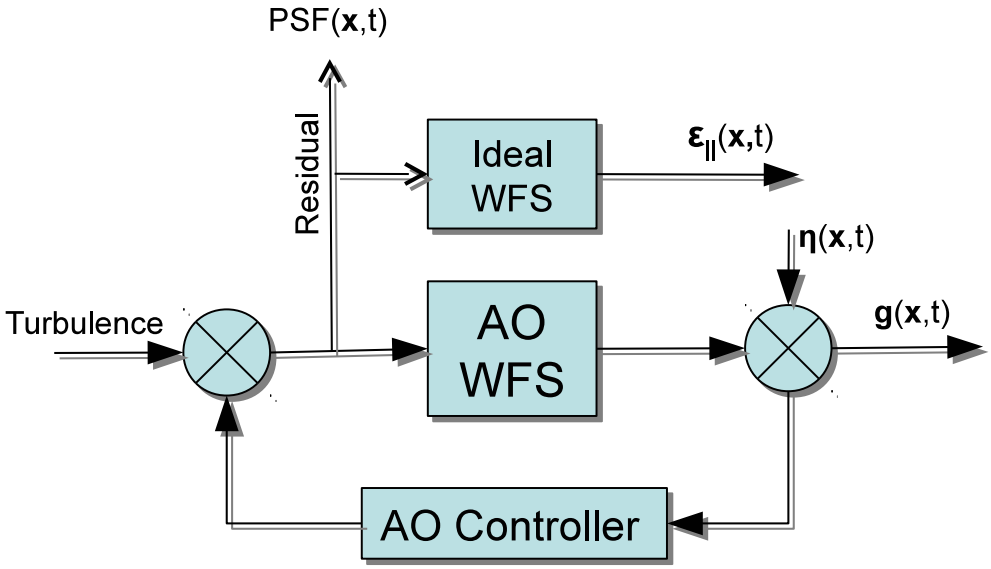

Fig. 1. Simplified scheme of PSF reconstruction with the AO WFS affected by measurement noise and aliasing and an ideal WFS that would give direct access to the residual phase after AO correction, here $\varepsilon_{\|}(\mathbf{x}, t)$. For the other variables, see text below.

The two-dimensional residual phase of a time-dependent disturbed wave-front is divided into low and high-order components

$$\phi(\mathbf{x}, t) = \varepsilon_{\|}(\mathbf{x}, t) + \phi_{\perp}(\mathbf{x}, t) \tag{1}$$

According to [Véran et al., 1997] the wave-front measurements given by the HS-WFS can be modelled as follows (spatial and temporal dependence omitted):

$$\mathbf{g} = \Gamma\varepsilon_{\|} + \eta + \mathbf{r} \tag{2}$$

where Γ is pupil-plane phase-to-wavefront matrix (WFS-specific), η is the measurement noise that includes photon and read-out noise and $\mathbf{r}$ is the remaining error, mostly associated to aliasing.

Suppose $R \triangleq \Gamma^{\dagger}$ can be computed explicitly . $\Gamma^{\dagger}$ is the pseudo-inverse of Γ to obtain an estimate of the phase in the pupil from closed-loop telemetry. Assuming noise processes η and $\mathbf{r}$ independent and also independent from phase, the phase covariance matrix is hence

$$\Sigma_{\varepsilon_{\|}} = \left\langle \varepsilon_{\|}\varepsilon_{\|}^{\mathsf{T}} \right\rangle = R\left\langle \mathbf{g}_0\mathbf{g}_0^{\mathsf{T}} \right\rangle R^{\mathsf{T}} = R\left(\Sigma_{\mathbf{g}} - \Sigma_{\eta} - \Sigma_r - 2\Gamma\left\langle \varepsilon_{\|}\mathbf{r}^{\mathsf{T}} \right\rangle\right) R^{\mathsf{T}} \tag{3}$$

where the de-noised measurements are given by $\mathbf{g}_0 = \mathbf{g} - \eta - \mathbf{r}$. $\Sigma_{\mathbf{g}} = \left\langle \mathbf{g}\mathbf{g}^{\mathsf{T}} \right\rangle$ is the covariance of the noisy measurements, $\Sigma_{\eta} = \left\langle \eta\eta^{\mathsf{T}} \right\rangle$ is the covariance of the measurement noise and likewise $\Sigma_{\mathbf{r}} = \left\langle \mathbf{r}\mathbf{r}^{\mathsf{T}} \right\rangle$ is the covariance of the remaining error.

An important difference to classical systems needs be underlined: unlike classical systems where the AO-loop real-time reconstructor coincides with the PSF reconstructor – regardless of whether it is

a minimum-variance (MV) or a least-squares (LS) one – in the current approach R is not to be confused with the tomographic reconstructor relating several WFS measurement to several layers for real-time estimation of phase in the volume. Instead R is a pupil-plane reconstructor for a single on-axis LGS WFS, which will make the phase estimation differ from the AO-loop estimation, a potential drawback of this method as will be shortly seen.

If the AO loop were to use a LS reconstructor, then the closed-loop gradients would only be nulled if $\Gamma\phi_{\|} = -\mathbf{r}$ for reasonably fast temporal frame-rates [Véran et al., 1997]. Subsequently, the aliasing covariance matrix would be well approximated by

$$-\Sigma_r - 2\Gamma\left\langle\varepsilon_{\|}\mathbf{r}^{\mathsf{T}}\right\rangle \approx \Sigma_r \tag{4}$$

and with a model for the noise covariance matrix, the residual covariance in Eq. (3) could be determined. Section 3.1 details how the SF is obtained from covariance matrices.

3 PSF reconstruction for tomographic AO systems with many degrees-of-freedom

3.1 Estimate the PSF from covariance matrices

The phase structure function (SF) is given by

$$D_\phi(\mathbf{x},\mathbf{x}') \triangleq \left\langle\|\phi(\mathbf{x}) - \phi(\mathbf{x}')\|^2\right\rangle \tag{5}$$

For a point-wise discretization of the phase, the phase SF can be straightforwardly computed from the phase covariance matrices Σ elements as follows

$$D_\phi[k,l] = \Sigma_\phi[k,k] + \Sigma_\phi[l,l] + 2\Sigma_\phi[k,l] \tag{6}$$

which circumvents the use of the commonly-called U_{ij} functions that are rather cumbersome to compute, in particular for ELT-sized systems. For example, for NFIRAOS, there would represent $(3125)^2$ U_{ij} functions to compute the SF from phase in the DM influence-functions-spanned vector space. These U_{ij} functions, despite the locality of the influence-functions, turn out to be full matrices (as opposed to sparse matrices) and thus unadapted to efficient PSF reconstruction.

In the full featured PSF reconstruction, we compute the LE OTF directly from the SF without making any pupil averaging approximation, remaining in SF space until we get the TTR science SF. To illustrate the results of the PSF reconstruction of a single LGS at the centre of the field we compute an average SF from which the OTF can be computed as

$$\overline{O}(\mathbf{k}) = e^{-\frac{1}{2}\overline{D}_{\varepsilon_{\|}}(\mathbf{x})}O_{\perp}(\mathbf{k})O_{tel}(\mathbf{k}) \tag{7}$$

where $\overline{D}_{\varepsilon_{\|}}(\mathbf{x})$ is the average residual phase SF, $O(\mathbf{k})_{\perp}$ is the fitting error OTF and $O(\mathbf{k})_{tel}$ is the telescope OTF. The PSF is readily computed from the OTF by Fourier transform.

3.2 Minimum-variance AO systems

A first remarkable difference to classical PSF reconstruction related to the use of minimum-variance (MV) phase reconstructors. The latter will filter out some of the measurement and aliasing errors, avoiding their propagation through the loop. Therefore, the approximation of Eq. (4) no longer stands. A MV AO loop is not a zero-measurement seeking loop.If the aliasing were totally filtered out based on the *a-priori* model of the turbulence, then the covariance $\left\langle\phi_{\|}\mathbf{r}^{\mathsf{T}}\right\rangle$ tends to zero and one would have in this limiting case $-\Sigma_r - 2\Gamma\left\langle\phi_{\|}\mathbf{r}^{\mathsf{T}}\right\rangle \approx -\Sigma_r$ instead of Eq. (4) as the approximation above, under the

hypothesis of least-squares reconstruction, would lead to. The particulars are further discussed below in §3.3.

Furthermore matrix Γ is ill-conditioned and differs from the tomographic reconstructor used in the loop. Its inversion will also require special attention. A customised regularisation is proposed in §3.4. For the noise and fitting errors, the commonly assumptions apply and no special treatment is required that is specific to MV tomographic systems.

3.3 Aliasing error

For a HS-WFS that spatially samples the average gradient of the wave-front every d meters, the open-loop aliasing power-spectral density (PSD) is a stationary process conveniently represented in the Fourier domain. An analytical expression can be found in [Flicker, 2007]

$$\mathbf{\Phi}_{alias,OL}(\mathbf{f}) = \frac{0.0229}{sinc(d\mathbf{f})} \sum_{\mathbf{m}\neq(0,0)} \frac{\bar{\mathbf{\Phi}}}{\left(|\mathbf{f}|^2 + 1/L_0^2\right)^{11/6}} |\tilde{\mathbf{R}}|^2 \mathbf{f}_\mathbf{m}^2 sinc(d\mathbf{f}_\mathbf{m}) \sum_{l=1}^{N_l} r_{0,l}^{-5/3} sinc(\mathbf{f}_\mathbf{m} \cdot \mathbf{v}_l T) \tag{8}$$

with $\mathbf{f}_\mathbf{m} \triangleq \mathbf{f} - \mathbf{m}/d$ the 2D aliased frequencies ; $\mathbf{f}$ is a two-dimensional frequency vector, D is the telescope diameter, d the sub-aperture diameter, N_l the number of layers in the atmosphere, v_l the windspeed per layer , $r_{0,l}$ the layered fractional Fried parameter, L_0 the outer scale of turbulence, T sampling time and $\bar{\mathbf{\Phi}}$ is the piston-removed wave-front $\bar{\mathbf{\Phi}} = \mathbf{\Phi}\left[1 - \left|\frac{2J_1(\pi \mathbf{f} D)}{\pi \mathbf{f} D}\right|^2\right]$ where J_1 is a Bessel function of the first kind. In closed-loop, the aliasing becomes

$$\mathbf{\Phi}_{alias,CL}(\mathbf{f}) = \mathbf{\Phi}_{alias,OL}(\mathbf{f}) \frac{g^2}{1 - 2acos(b_l) + a^2} \tag{9}$$

where $a = 1 - g, b_l = i2\pi \mathbf{f}_\mathbf{m} \cdot \mathbf{v}_l T$ with g the type-I servo integrator gain used in the LGS loop.

The MV reconstructor in the spatial frequency domain writes

$$\tilde{\mathbf{R}} \triangleq \frac{-i\mathbf{f}}{\|\mathbf{f}\|^2 + \mathbf{\Theta}/\mathbf{\Phi}} \tag{10}$$

where $\mathbf{\Theta}$ is the PSD of the noise and $\mathbf{\Phi}$ the PSD of the uncorrected phase – the LS reconstructor is readily obtained from Eq. (10) setting $\mathbf{\Theta}/\mathbf{\Phi} = 0$. Figure 2 shows a radial cut of a two-dimensional PSD for the aliasing error obtained with a LS reconstructor and with a MV reconstructor.

3.4 Pupil-plane reconstructor

In the general case, the phase reconstructor is obtained by inverting the phase-to-slopes matrix Γ in Eq. (2), using the truncated singular value decomposition method.

However, as the simulations early showed, R is severely ill-conditioned and cannot be obtained so easily. Instead, a regularisation factor was introduced to render the inversion better conditioned. Such regularisation consists of a second derivative functional that stems from the residual after applying a MV reconstructor. Figure 3 depicts a radial cut of the spatial PSD obtained before and after reconstruction. One can easily observe that the residual corresponds almost in its entirety to the noise propagated through the reconstruction and that this PSD is close enough to the $\propto \mathbf{f}^{-2}$ power law.

Under these considerations, the following quadratic penalty is introduced to get

$$R = \left(\Gamma^\mathsf{T}\Gamma + \gamma \Sigma_{\varepsilon_\parallel}^{-1}\right)^{-1} \Gamma^\mathsf{T} \tag{11}$$

with γ a scalar factor to further balance the relative weight of the regularisation and $\Sigma_{\varepsilon_\parallel}$ the Fourier transform of the residual phase PSD (using the Wiener-Khinchine theorem, one gets the covariance matrix).

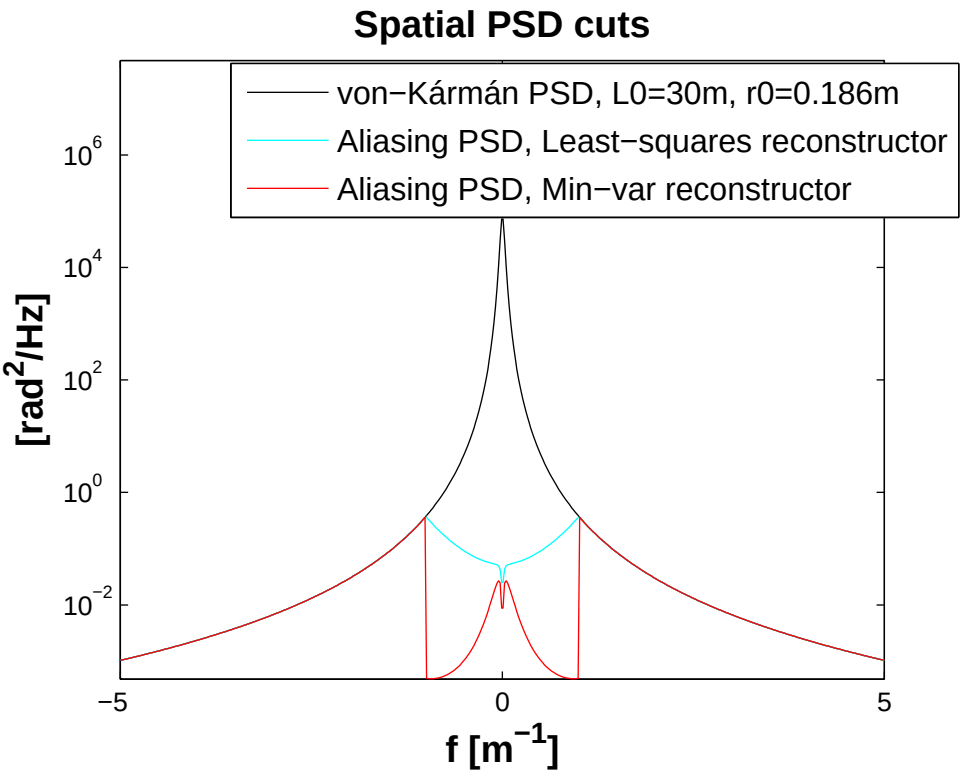

Fig. 2. Radial cuts of the uncorrected phase PSD, the aliasing given by Eq. (8) for a least-squares reconstructor (*i.e.* with $\boldsymbol{\Theta}/\boldsymbol{\Phi} = 0$ in Eq. (10)) and for a MV reconstructor with $\boldsymbol{\Theta}/\boldsymbol{\Phi} \neq 0$. The aliased frequencies within the $\mathbf{f} \leq 1/(2d)$, $d = 0.5$m is neatly visible, with the MV reconstructor mitigating a quite substantial amount of the total aliasing that would be otherwise propagated with a LS reconstructor.

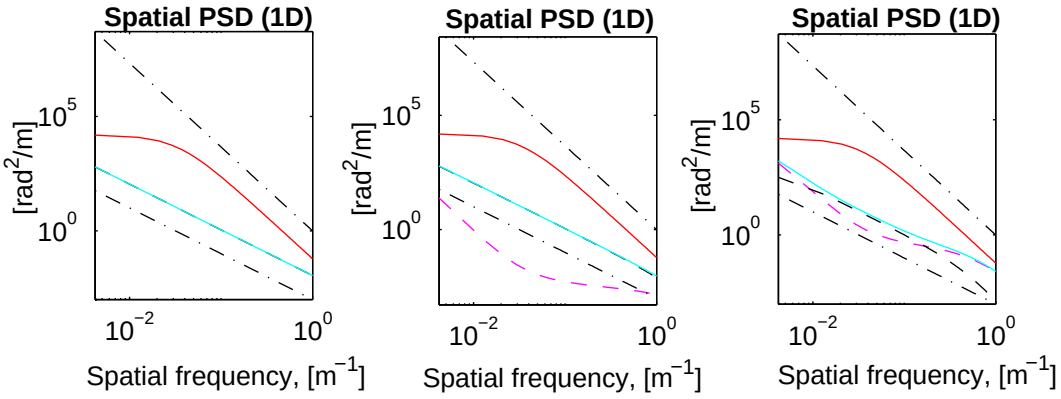

Fig. 3. Radial cuts of the uncorrected phase PSD (red), the phase error (magenta), noise propagated (dashed black) and the residual phase which is equal to phase error + noise propagated (cyan). Left: LS reconstructor, centre and right: MV reconstructor with two different factors on the regularisation strength. Dotted-dashed lines are a $\propto f^{-11/3}$ (top) and $\propto f^{-2}$ (bottom) power laws.The total residual phase follows a $\sim \mathbf{f}^{-2}$ power law, which suggests the regularisation can consist of a quadratic penalty.

3.5 Fitting-error

For the fitting error the common assumptions are done as for the single-conjugate AO systems with least-squares reconstructors. Fitting refers to the component of the phase that the AO systems cannot correct for. If $\mathbf{\Phi}_{\parallel}^{DM}(\mathbf{f})$ is the phase in DM space that the DM is able to correct for, then

$$\mathbf{\Phi}_{\perp}(\mathbf{f}) = \mathbf{\Phi}(\mathbf{f}) - \mathbf{\Phi}_{\parallel}^{DM}(\mathbf{f}) = \mathcal{H}(\mathbf{f})\mathbf{\Phi}(\mathbf{f}) \tag{12}$$

where

$$\mathcal{H}(\mathbf{f}) \triangleq 1 - \frac{\mathbf{\Phi}_{\parallel}^{DM}(\mathbf{f})}{\mathbf{\Phi}(\mathbf{f})} \tag{13}$$

and $\mathbf{\Phi}_{\perp}(\mathbf{f})$ is the higher-order component from Eq. (1). For a realistic AO system, $\mathbf{\Phi}_{\parallel}^{DM}(\mathbf{f})$ is obtained by filtering the phase PSD $\mathbf{\Phi}(\mathbf{f})$ by the modulus squared of the Fourier transformed translation-invariant DM influence function.

3.6 Measurement noise

The noise contribution is obtained from the RTC on-axis LGS WFS signal-to-noise ratio, detector model and centroiding algorithm used during science exposure. In the simulation-only case presented here, the measurement noise covariance matrix is perfectly know such that using noise-free measurements or de-noised measurements (using the former in Eq. 3) leads to the exact same results, provided the telemetry is accumulated over a large enough timespan to ensure statistical convergence – in our case 2 seconds of real-time data proved sufficient. For an overview of estimation techniques, refer to [Véran, 2007] and the bibliographic references therein.

4 Numerical results

Without further detailing the (extensive list of) parameters of NFIRAOS simulation, for the purposes of PSF reconstruction the triplet $(d, r_0, L_0) = (1/2, 0.186, 30)m$ is used.

Although the Fourier-domain approach seems attractive to model all the terms required for PSFR, the noise is not spatially invariant (LGS spot elongation radially, 'x' and 'y' correlations) which mean that a Fourier representation will no longer apply to the AO terms. Instead, 3 different full NFIRAOS MAOS simulations are run with the actual tomographic AO reconstructor to probe the aliasing, fitting and residual phase independently. For a LS reconstructor, $\int \Phi_{alias}(\mathbf{f})\mathrm{d}\mathbf{f} = 0.073(d/r_0)^{5/3}$ [Ellerbroek, 2005], whereas with MAOS a slightly smaller value is obtained which follows the discussion of §3.3: for the MV reconstructor $\int \Phi_{alias}(\mathbf{f})\mathrm{d}\mathbf{f} = 0.0478(d/r_0)^{5/3}$, which represents roughly 2/3 of the former, *i.e.* 1/3 of the LS aliasing is filtered out by the MV reconstructor. The total error is 39.67 nm rms, lower than the 49 nm rms that would be used if the approximation of Eq. (4) were adopted.

The fitting error for purely sinus-cardinal functions is $\int \mathbf{\Phi}_{\perp}(\mathbf{f})\mathrm{d}\mathbf{f} = 0.23(d/r_0)^{5/3}$ [Ellerbroek, 2005]. Using MAOS end-to-end simulator, $\int \mathbf{\Phi}_{\perp}(\mathbf{f})\mathrm{d}\mathbf{f} = 0.29(d/r_0)^{5/3}$ for bilinear splines and $\int \mathbf{\Phi}_{\perp}(\mathbf{f})\mathrm{d}\mathbf{f} = 0.24(d/r_0)^{5/3}$ for bicubic splines with 20% cross-coupling, a sign that the bicubic influence functions in the half-pitch sheared lower and upper DMs behave roughly as the best *sinc* functions. The fitting contributes with 78.37 nm rms.

Using the previous results, Fig. 4 depicts the achieved OTF results with the estimated Strehl-ratio in J-band higher than the simulated one by ~ 0.3%.

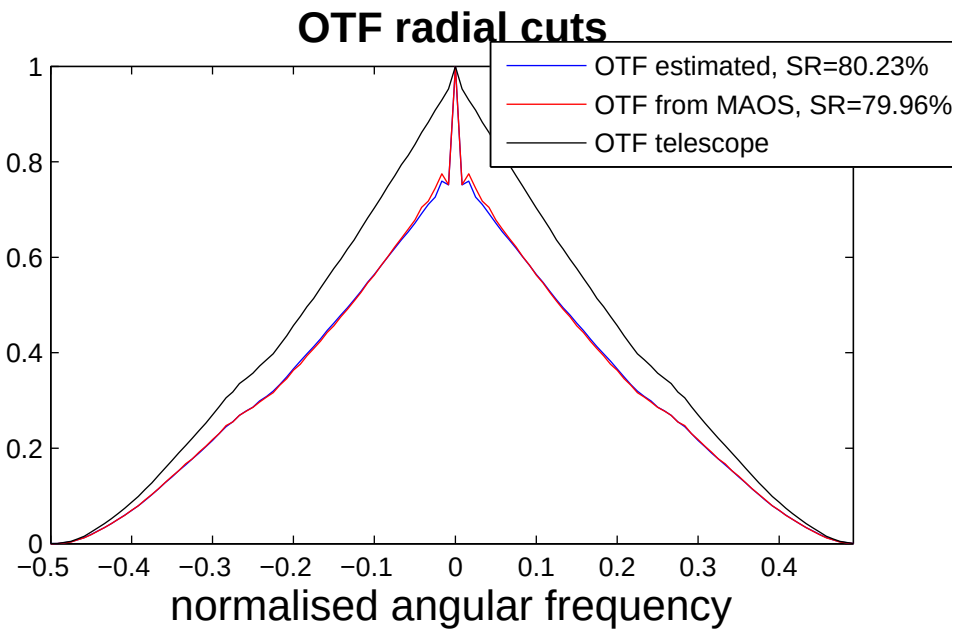

Fig. 4. Radial cuts of the uncorrected OTF, the estimated from telemetry and the one obtained from MAOS, the high-fidelity AO simulator.

5 Outlook

A computationally sound method to reconstruct the on-axis LGS PSF for laser-tomographic systems is presented. The results achieved are then plugged into a more general approach to fully estimate the science PSF for LGS-MCAO systems in [Gilles et al., 2011].

Using a zonal approach, a much faster PSF estimation is possible, circumventing the computing of the commonly-used U_{ij} functions which would be impractical for ELT-sized tomographic AO systems.

It has been shown that the choice of certain parameters may be quite delicate as is the case of the regularisation parameter to be used on the on-axis pupil-plane reconstructor. Such estimation still lacks some robustness and although preferable, a fully analytical estimation seems out of scope due to spatial variance of the terms involved, in particular noise due to spot elongation. Therefore a simulation-based method has been adopted based on the MAOS high-fidelity multi-threaded *C* code. This code has been extensively used to populate the precomputed look-up tables that we are presently using (for the regularisation, aliasing and fitting factors), something we will further work on to better balance the unavoidable compromise between parameter choice and overall PSF estimation quality.

References

[Ellerbroek, 2005] Ellerbroek, B. L. (2005). Linear systems modeling of adaptive optics in the spatial-frequency domain. *J. Opt. Soc. Am. A*, 22(2):310–322.

[Flicker, 2007] Flicker, R. (2007). Analytical evaluations of closed-loop adaptive optics spatial power spectral densities. Technical report, W. M. Keck Observatory.

[Gilles et al., 2011] Gilles, L., Ellerbroek, B. L., Wang, L., Veran, J.-P., and Correia, C. (2011). Long exposure point spread function reconstruction for laser guide star multi conjugate adaptive optics. In *2nd AO4ELT Conference - Adaptative Optics for Extremely Large Telescopes proceedings*.

[Véran, 2007] Véran, J.-P. (2007). PSF Reconstruction for Advanced AO Systems. In *Adaptive Optics: Analysis and Methods/Computational Optical Sensing and Imaging/Information Photon-*

ics/Signal Recovery and Synthesis Topical Meetings on CD-ROM, page ATuA1. Optical Society of America.

[Véran et al., 1997] Véran, J.-P., Rigaut, F., Maître, H., and Rouan, D. (1997). Estimation of the adaptive optics long-exposure point-spread function using control loop data. *J. Opt. Soc. Am. A*, 14(11):3057–3069.

[Wang et al., 2011] Wang, L., Ellerbroek, B. L., and Gilles, L. (2011). Analysis of the improvement in sky coverage for mcao systems obtained using minimum variance split tomography. *J. Opt. Soc. Am. A*.